Journal for ImmunoTherapy of Cancer

Mast cell-T cell axis alters development of colitis-dependent and colitis-independent colorectal tumours: potential for therapeutically targeting via mast cell inhibition

Juliana Y Sakita,[1] Jefferson Elias-Oliveira,[2] Daniela Carlos,[2] Emerson de Souza Santos,[3] Luciana Yamamoto Almeida,[4] Tathiane M Malta,[3] Mariângela O Brunaldi,[5] Sergio Albuquerque ,[3] Cleide Lúcia Araújo Silva,[6] Marcus V Andrade,[7] Vania L D Bonato,[2] Sergio Britto Garcia,[5] Fernando Queiroz Cunha,[8] Guilherme Cesar Martelossi Cebinelli,[8] Ronaldo B Martins,[9] Jason Matthews,[10,11] Leandro Colli,[12] Francis L Martin,[13,14] Sergio A Uyemura,[3] Vinicius Kannen [1,10]

To cite: Sakita JY, Elias-Oliveira J, Carlos D, *et al*. Mast cell-T cell axis alters development of colitis-dependent and colitis-independent colorectal tumours: potential for therapeutically targeting via mast cell inhibition. *Journal for ImmunoTherapy of Cancer* 2022;**10**:e004653. doi:10.1136/jitc-2022-004653

► Additional supplemental material is published online only. To view, please visit the journal online (http://dx.doi.org/10.1136/jitc-2022-004653).

SAU and VK are joint senior authors.

Accepted 07 September 2022

For numbered affiliations see end of article.

Correspondence to
Dr Vinicius Kannen;
vinicius.kannen@utoronto.ca

ABSTRACT

Background Colorectal cancer (CRC) has a high mortality rate and can develop in either colitis-dependent (colitis-associated (CA)-CRC) or colitis-independent (sporadic (s)CRC) manner. There has been a significant debate about whether mast cells (MCs) promote or inhibit the development of CRC. Herein we investigated MC activity throughout the multistepped development of CRC in both human patients and animal models.

Methods We analyzed human patient matched samples of healthy colon vs CRC tissue alongside conducting a The Cancer Genome Atlas-based immunogenomic analysis and multiple experiments employing genetically engineered mouse (GEM) models.

Results Analyzing human CRC samples revealed that MCs can be active or inactive in this disease. An activated MC population decreased the number of tumor-residing CD8 T cells. In mice, MC deficiency decreased the development of CA-CRC lesions, while it increased the density of tumor-based CD8 infiltration. Furthermore, co-culture experiments revealed that tumor-primed MCs promote apoptosis in CRC cells. In MC-deficient mice, we found that MCs inhibited the development of sCRC lesions. Further exploration of this with several GEM models confirmed that different immune responses alter and are altered by MC activity, which directly alters colon tumorigenesis. Since rescuing MC activity with bone marrow transplantation in MC-deficient mice or pharmacologically inhibiting MC effects impacts the development of sCRC lesions, we explored its therapeutic potential against CRC. MC activity promoted CRC cell engraftment by inhibiting CD8+ cell infiltration in tumors, pharmacologically blocking it inhibits the ability of allograft tumors to develop. This therapeutic strategy potentiated the cytotoxic activity of fluorouracil chemotherapy.

Conclusion Therefore, we suggest that MCs have a dual role throughout CRC development and are potential druggable targets against this disease.

WHAT IS ALREADY KNOWN ON THIS TOPIC

⇒ The role of mast cells (MCs) in colorectal cancer (CRC) is controversial as they can either promote or inhibit it. Studying this issue may reveal druggable targets for oncostatic therapies.

WHAT THIS STUDY ADDS

⇒ Our study shows that an MC-lymphocyte axis alters the development of both CA-CRC and sporadic CRC. However, several immune mechanisms can also change MCs' function and CRC development. Moreover, pharmacologically inhibiting MC activity blocks the growth of CRC and melanoma tumors. This therapeutic strategy can be combined with a chemotherapeutic compound.

HOW THIS STUDY MIGHT AFFECT RESEARCH, PRACTICE OR POLICY

⇒ Our findings define specific conditions in which MCs can promote or block CRC development. They also highlight MCs as a versatile druggable target against melanoma and CRC.

INTRODUCTION

Mast cells (MCs) have been suggested to play a pivotal yet complex role in several immune-mediated reactions in the body.[1–3] Bone marrow releases immature MCs that migrate towards their patrolling sites that are then activated according to immediate region-specific needs. Also, MCs synthesize inflammatory factors towards antigens binding to the Fc region of IgE coating their membrane.[2–4]

In human colorectal cancer (CRC), a reduced MC population has been associated

with a good prognosis, while elevated numbers appear to be associated with poorer disease outcomes.[5 6] Conversely, there have also been reports suggesting that increased MC numbers in tumors promote patient survival rates.[7 8] In carcinogen-exposed animal models, which resemble the development of sporadic CRC (sCRC), MC deficiency reduced tumor burden.[9] Pharmacologically inhibiting MCs' activity decreased CRC risk also.[10]

Other research groups have suggested that MCs promote the development of colitis-associated CRC (CA-CRC) in mice.[11 12] Haribabu and colleagues reported that MC deficiency promotes the development of colon tumors in mice carrying a heterozygous mutation in the *adenomatous polyposis coli* ($Apc^{Min/+}$) gene; thus, MCs might orchestrate an anticancer immunological reaction during the development of intestinal tumorigenesis.[13] Sinnamon *et al* demonstrated similar observations that MC deficiency increases tumor numbers in $Apc^{Min/+}$ mice.[14]

Whether the MC activity can differentially alter the development of CA-CRC and sCRC lesions remains unknown. We have thus challenged the hypothesis that MC activity alters and can be altered by different immune reactions. Our findings not only confirm that a MC-T cell axis alters the development of CA-CRC and sCRC tumors but that its potential can be pharmacologically harnessed to treat CRC in combination with a standard chemotherapeutic compound.

MATERIALS AND METHODS

Human samples and immunogenomic analysis

According to the Declaration of Helsinki for the research use of previously collected human biospecimens in minimal risk studies, this Research Ethics Committee waived the patient informed consent. None of the patients underwent chemotherapy or radiotherapy prior to sample collection. Coded tissue samples ensured patient confidentiality.

Also, we performed an immunogenomic analysis based on 604 CRC cases from The Cancer Genome Atlas (TCGA). It investigated the immune cell population estimated by CIBERSORT,[15] and the immune features that our previous report described.[16] Additionally, we selected the TCGA CRC samples classified as 'genome stable subtype' and divided them in two groups based on the frequency of activated MC by setting up a dichotomy comparing the top quarter (high MC activated frequency, HMCA) against the bottom quarter (low MC activated frequency, LMCA). The samples with intermediary frequency were excluded from the analysis.

Mouse experiments

The Research Ethics Committee for Animal Use of the School of Pharmaceutical Sciences of Ribeirao Preto of the University of Sao Paulo approved the current study (22.1.233.60.2). The following mouse strains were purchased from the Jackson Laboratories (USA): $Kit^{W/sh}$ (#012861), $Kit^{W/W\text{-}v}$ (#100410), *B2m* knockout (KO; #002087), *Ciita* KO (#003239), *Il6* KO (#002650), NOD (#001976), NOD-*scid*γ (#005557), C57BL/6J (#000664; named herein Kit^{B6}, *B2m*WT, or *Ciita*WT), BALB/cJ (#000651; named herein *St2*WT), C57BL/6-Tg(CAG-EGFP)131Osb/LeySopJ (#006567; named herein $Kit^{B6\text{-}Tag(CAG\text{-}EGFP)}$), and *Rag1* KO (#002216). The *St2*KO mouse strain was developed and donated by Dr Andrew McKenzie.[17]

Cell culture, co-culture, and allograft CRC model

A murine CRC cell line (MC38) was cultured (±95% humidity; 37°C; 5% CO_2) in Dulbecco's Modified Eagle Medium (D5030; 10% foetal bovine serum, 12103C; 100 U/mL penicillin-streptomycin, P0781; 10 mM sodium pyruvate, P5280; Sigma-Aldrich, USA).

To harvest tumor-primed MCs, Kit^{B6} mice were intraperitoneally (i.p.) injected with MC38 cells (1×10^6). Following 7 days from this procedure, MCs were isolated from the peritoneal cavity according to our previous description.[18] Tumor-primed MCs were co-cultured with MC38 cells at a ratio of 1:10.

MC38 cells (2×10^6) were subcutaneously injected to induce allograft tumors in both $Kit^{W/sh}$ and Kit^{B6} mice. Tumors grew for 14 days and were monitored with a caliper. Treatments started from the seventh day onwards. Treatments were saline, cromolyn (CA; Sigma-Aldrich; C0399; 25 mg/ kg/ day,[19] and 5-fluorouracil (5-FU; Libbs Farmaceutica Ltda, Sao Paul, Brazil; 70 mg/ kg once every 3 days.[20]

Colon tumorigenic mouse models

The CA-CRC protocol consisted of a single i.p. injection of azoxymethane (AOM; 10 mg/kg; Sigma-Aldrich; A5486) followed by three cycles of 2% dextran sulfate sodium (Sigma-Aldrich; 42867.[21] Experiments were ended in a CO_2 chamber (10th week).

The sCRC protocol consisted of 6 i.p. injections of AOM throughout 6 weeks. Tumors were detected after other 18 weeks.[21] Early tumorigenic lesions (APL) were detected after 6 weeks from the sixth AOM exposure. DNA damage can be studied after 3 days and single APLs (PL) after 1 week from the sixth AOM injection. Our protocol of 3 i.p. AOM injections followed by 3 days or 3 weeks was also applied.[22]

Bone marrow transplantation

To rescue MC deficiency, $Kit^{W/sh}$ mice and their counterparts underwent a single lethal dose of whole-body irradiation (IR; RS-2000 Biological Research Irradiator [Rad Source, Kansas City, MO, US]; 7 Gy). After 12 hours, IR-exposed mice received 1×10^7 freshly isolated mouse bone marrow cells expressing enhanced green fluorescent protein (EGFP) from $Kit^{B6\text{-}Tag(CAG\text{-}EGFP)}$ mice.[23] After other 6 weeks, bone marrow transplantation (BMT) was confirmed by counting EGFP cells in flow cytometry (Guava easyCyte 8HT [MerkMillipore, Burlington, MA, USA]; InCyte 2.7 software). Then, mice underwent sCRC protocol.

qPCR

The RNeasy Mini Kit (74104; Qiagen, DE) was used to prepare RNA samples. Then, cDNA synthesis followed the manufacture's guideline for the SuperScript III Reverse Transcriptase kit (Thermo Fisher Scientific, USA; 18080093). Online supplemental table 1 and 2 show probes and primers, respectively. Data were collected and analyzed using an Eppendorf Mastercycler RealPlex2 system (Eppendorf, DE). The fold-change (FC) between reaction control, experimental control, and target groups was calculated using the $2^{-\Delta\Delta Ct}$ method (*Gapdh* as a housekeeping gene).

Flow cytometry

According to the manufacturer's guideline (Thermo Fisher Scientific, USA), the Annexin V/ 7AAD kit (#88-8006-74) was used to analyze viability and apoptosis. Also, colonic lymphocytes, tumor immune cellular populations, and tumor cells were isolated as we have described previously.[24 25] Then, samples were incubated with antibodies against CD45-FITC (1:250), CD45-APC (1:250), CD45-BV421 (1:300), CD117-PE-Cy7 (1:250), FcεRI-PE (1:250), CD8a-PE (1:300), CD3-FITC (1:250), CD4-FITC (1:250), and FOXP3-APC (1:300; online supplemental table 3). Cellular viability was checked by 7AAD (#A1310; Thermo Fisher Scientific) or FVS-APC Cy-7 (#565388; BD Biosciences). The data acquisition was performed on FACSVerse (BD Biosciences) and analysis carried out by the FlowJo software (FlowJo LLC, USA). Lymphocytes were determined as $CD4^+$, $CD4^+FOXP3+$, $CD8^+$, and $CD8^+CD3^+$ gated from singlet viable $CD45^+$ cells. MCs were determined as CD45+FcεRI+CD117+ cells. Values are given as percentage.

Clonogenic assay

For decades the clonogenic assay has been used to test the number of cancer cell colonies in different experimental settings.[26] It can also be applied in co-culturing systems.[27] After tumor-primed MCs were co-cultured with MC38 cells for 5 days, colonies were fixed and stained with 0.2% crystal violet solution. The well area normalized the number of colonies.

Histopathological analysis and multiplex immunohistochemistry

As previously reported,[28] 4 µm paraffin-embedded tissue sections were stained with toluidine blue (Sigma-Aldrich; 89640) before determining the density of MCs *per* sample area (iTB; Axio Imager M2 [Carl-Zeiss, DE]). To validate this analysis (iTRY), immunohistochemistry (IHC; Picture-Max Dab Kit; Thermo Fisher Scientific, USA; 878983) stained samples following manufacturer's instructions (anti-MC tryptase [TRY; 1:100; ab2378], ABCAM, USA;).

Following our previous description,[22] tumors and preneoplastic tissue samples underwent H&E staining and analysis (lesions *per* mm^2). IHC stained samples with primary antibodies (online supplemental table 1) for analysis (number of positive *per* crypt).

A multiplex IHC was performed following our protocol.[22] Reactivity to primary antibodies (online supplemental table 3; online supplemental figure 1) was determined by a Vector AEC Substrate kit (Vector Laboratories, USA; SK-4200). Stained tissue slides were scanned using an Aperio ImageScope AT system (Leica Biosystems, DE). Image processing and visualization were carried out using ImageScope software (Leica Biosystems).

RNAseq panel analysis

To prepare RNA samples, we used Qiagen RNeasy (#74106) and Qiagen RNase-free DNase kits (#79254). The RNA integrity was analyzed by Agilent Bioanalyzer RNA 6000 Nano kit (Agilent Technologies, USA; #5067–1511). The cDNA libraries were built with QIAseq Targeted RNAseq Mouse Immuno-Oncology panel (#333005) and QIAseq Targeted RNA 96-Index I kits (#333117). The Agilent Bioanalyzer DNA 1000 Assay (#5067–1504) assessed libraries quality and size. The QIAseq Library Quant Assay Kit (#333314) quantified libraries before the Illumina MiSeq Reagent Kit v3 (150 cycles; Illumina Inc., USA; #15043894) was applied for sequencing them in a MiSeq Sequencing System. Datasets (GSE 146786) were analyzed with the R package DESeq2.[29]

Immunoblotting analysis

According to our previous report,[22] immunoblotting analyses were performed. Following cold protein extraction (RIPA Buffer, R0278; phosphatase inhibitors, P0044; protease inhibitor, P2714; Sigma-Aldrich), protein concentration was determined (Pierce BCA Protein Assay Kit, 23225; Thermo Fisher Scientific). Any kD Mini-PROTEAN TGX Stain-Free Protein Gels (#4568123; Bio-Rad Laboratories, USA) were used for electrophoresis. Then, we used the Bio-Rad Trans-Blot Turbo Mini Nitrocellulose Transfer Packs (#1704158) together with the Bio-Rad Trans-Blot Turbo Transfer System. Next, membranes were incubated at 4°C overnight with primary antibodies (online supplemental table 3).

Statistical analysis

The R software was applied for the TCGA-based immunogenomic analysis.[30] Also, we computed the Pearson correlation between immune features and MC populations. A two-tailed T-test was used to analyze the frequency of immune cell populations/signatures between CRC samples with low (LMCA) and HMCA frequencies.

The R software was also applied for analyzing the RNAseq datasets. After the data normalization by DESeq2, the differential expression was calculated (p value adjust<0.05). Test t was used to analyze only two groups, while the one-way analysis of variance (ANOVA) (post hoc test Benjamini–Hochberg) was used to analyze more than two groups. The libraries used were: DESeq2, ComplexHeatmap, gplots and parallel.

Other datasets were analyzed in the GraphPad Prism 9.3 software (Graph Pad Software Inc., USA). The two-tailed Mann-Whitney's U test analyzed probabilities between two different groups. The one-way ANOVA test (Kruskal-Wallis' post hoc test) was applied to analyze experiments with more than two groups. The two-way ANOVA test (with Bonferroni's post hoc test) was applied to analyze different categorical independent endpoints with one dependent variable. A probability of $p<0.05$ was considered to be statistically significant.

RESULTS

The MC activity alters the lymphocyte population in human CRC cases

Analyzing matching samples of normal colon and CRC tissues reveals that MC numbers might increase or remain unchanged in this pathological condition when compared with normal colon tissue from the same patient (figure 1A,B). Furthermore, TCGA-based immunogenomic analysis of 604 CRC cases shows that MCs reside in tumors as either active or inactive units (figure 1C). We also observed that activated MCs negatively correlated with lymphocyte infiltration in CRC cases, whereas dormant MCs positively correlated with these cells (figure 1C). We further verified these observations by studying CRC cases in which activated MCs were present in either low (LMCA) or high numbers (HMCA). An HMCA appeared to decrease the number of tumor-residing CD8 T cells (figure 1D). Our observations confirm previous reports that MCs may alter the CRC development and CD8 T cell density in those lesions.

The MC activity impacts the development of colitis-dependent or colitis-independent tumors in mice

To test the idea that MCs can directly affect CRC cells, we first harvested high-MC numbers from Kit^{B6} mice bearing MC38 cell-induced ascites (figure 2A. Peritoneal MCs from MC38-bearing mice reduced proliferation of CRC cells in a co-culture model (figure 2B). MCs also promoted apoptosis in MC38 cells (figure 2C,D). Moreover, MCs decreased the number of MC38 colonies in a long-term co-culturing system (figure 2E,F).

To mechanistically explore MC activity throughout the multi-stage development of CRC, tumorigenesis was induced in mice in either a colitis-dependent (CA-CRC) or a colitis-independent fashion (sCRC).[21] Induction of CA-CRC in MC-deficient mice ($Kit^{W/sh}$) reduced tumor burden compared with counterparts, even with high-*Cd8* expression levels in those tumors (figure 3A,B). However, this experimental condition did not alter *Cd3* expression levels (Kit^{B6} – 1.0±0.1; $Kit^{W/sh}$ – 1.3±0.2; p=0.38). Histopathological analysis confirmed that MC-deficiency promoted a higher number of CD8+ cells in CA-CRC lesions (figure 3B). MC deficiency did not alter the *Cd11c* (Kit^{B6} – 0.6±0.08; $Kit^{W/sh}$ – 0.4±0.17; p=0.48) and *Cd4* levels (Kit^{B6} – 1.8±0.2; $Kit^{W/sh}$ – 2.5±0.6; p=0.48).

After mice underwent the sCRC induction protocol, we observed that MC deficiency promoted the development of sporadic colorectal tumors (figure 3C). In sCRC lesions, unlike the CA-CRC ones, MC deficiency did not alter the *Cd8* expression levels, nor the tumor infiltration of CD8 lymphocytes (figure 3D,E; Suppl online supplemental figure 2A). However, it decreased tumor *Cd3* expression levels (Kit^{B6} – 1.0±0.1; $Kit^{W/sh}$ – 0.6±0.1; p=0.04). By analyzing a proliferation biomarker, we observed proliferative rates did not change, significantly (figure 3E; online supplemental figure 2A–C).

To explore these findings, we performed an RNAseq analysis to investigate that MC deficiency alters several inflammatory responses (figure 3F**;** Suppl online supplemental table 4). MC deficiency upregulated the cytokine–cytokine receptor interaction pathway ($p=9.8^{-11}$; online supplemental table 5). Our findings suggest that MC activity varies according to the various factors inducing the development of colorectal tumors, as opposing results between CA-CRC and sCRC models demonstrate.

The MC-lymphocyte axis impacts the development of early tumorigenic events in the colon

Considering that MC deficiency may promote significant changes in the tumor microenvironment, we explored the hypothesis that MCs play a pivotal role in building this tumor microenvironment from the early tumorigenic steps onwards. First, we observed that the sCRC protocol increased the colonic CD8 T cell population during the development of the early tumorigenic steps in the colon (figure 4A; online supplemental figure 3). This finding led us to rationalize that major histocompatibility complex class I (MHCI) activity directly impacts the lymphocyte population.[31] When we induced early tumorigenic lesions in a MHCI deficiency model (*B2m* KO), we observed reduced *Cd8* expression levels but increased levels of MC biomarkers (MC protease 1, *Mcpt1* (epithelial); *Mcpt4* (stromal)[32]; figure 4B–E; online supplemental figure 1). Conversely, MHCII deficiency decreased the expression of *Mcpt1* and *Mcpt4* in the colon of AOM-exposed mice (figure 4F–I; online supplemental figure 4). To confirm that these early tumorigenic steps required a specific immune response to develop, they were induced in NOD-scidγ immunosuppressed mice. This experiment revealed that immunosuppression decreases the development of early tumorigenic lesions, epithelial cellular proliferation, and the number of MCs (online supplemental figure 5A–C).

As MC-deficient sCRC tumors had low *Il6* expression levels (figure 3F), a mouse Il6 deficiency model underwent induction of early tumorigenic lesions. This colonic Il6 deficient microenvironment decreased the development of early tumorigenic lesions and MC numbers (online supplemental figure 5D-E). Considering that we found that high-*Il33* levels occurs in MC deficient sCRC lesions (figure 3F) and a previous study has shown that the interleukin 33 receptor (*Il33r*) modulated MC-related tumorigenic effects [11], we induced early colon tumorigenic

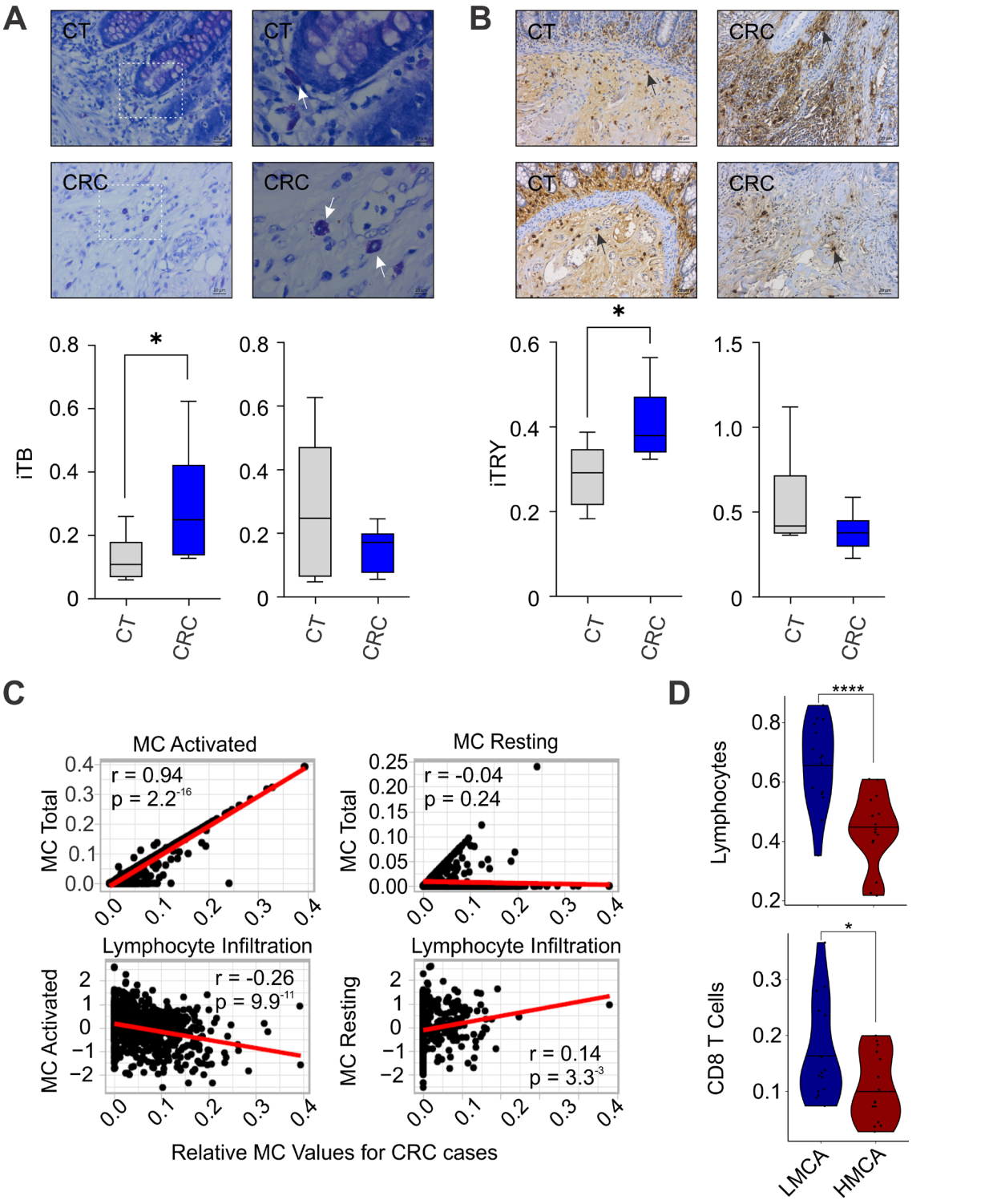

Figure 1 MC activity (MCA) effects in human CRC cases. (A) Representative images of MCs stained by TB (CRC or normal colon (CT) samples from the same patient; 40× (left-side) and 100× (right-side) magnification; sectioned lines indicate 100×magnified areas; arrows lead to positive cells). (B) Representative images of MCs stained by anti-tryptase antibody (TRY; 20× magnification; increased [upper-left] or unchanged (lower-left) MC numbers) in both CT and CRC samples. (A, B) MC density was found to be increased (A, n=16, *p=0.023; B, n=14, *p=0.026), or remain unchanged (A, n=22; B, n=12; p>0.05). (C) A Immune features (*y* axes; total MCs (upper panels), or leukocyte infiltration (lower panels)) vs MC activated (left panels) or resting fractions (right panels; *x* axes) for CRC cases from TCGA. (D) The CRC cohort positive for a MCA profile was divided in two groups of cases with low (LMCA) or high MCA values (HMCA). Lymphocytes and CD8 T cell levels are shown to be increased in LMCA group (****p=0.000105; *p=0.0284). Data are shown as the median, highest and lowest values, and upper and lower quartiles. Dots represent individual tumor samples. The Pearson correlation was applied. P values were calculated using two-tailed Mann-Whitney's U test. CRC, colorectal cancer; LMCA, low MC activated frequency; MC, mast cell; TB, toluidine blue; TCGA, The Cancer Genome Atlas.

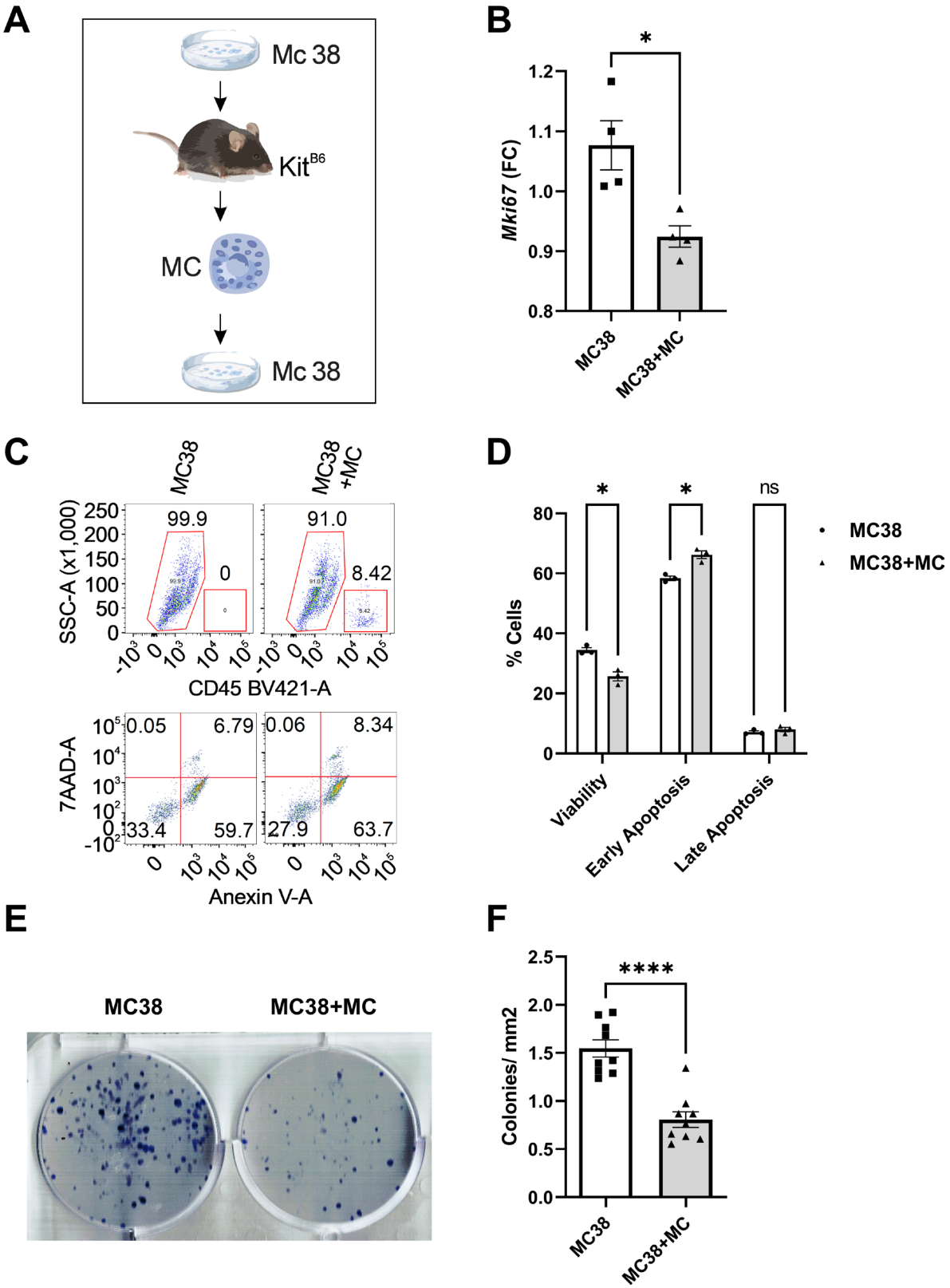

Figure 2 MCs induce apoptosis in murine CRC cells. (A) Tumor-primed MCs were isolated 7 days after KitB6 mice received a single i.p. injection of murine CRC cells (MC38). Once purified, tumor-primed MCs were co cultured with MC38 cells for 2 (B–D) or 5 days (E, F). (B) Gene expression analysis by qPCR for Mki67 (*, p<0.05). (C, D) Representative dot plots of flow cytometric analysis for gating CD45(-) cells or MC38. It was followed by viability and apoptosis analysis. Graph shows percentages of negative or positive MC38 cells for Anexin V (*, p<0.05). (E, F) Representative images of clonogenic assays. Graph shows the relative number of colonies for each group (****, p<0.001). Dots represent individual values together with mean±SEM. P values were calculated using two-tailed Mann-Whitney's and two-way ANOVA tests (Bonferroni's post hoc) tests. ANOVA, analysis of variance; CRC, colorectal cancer; MCs, mast cells; ns, not significant.

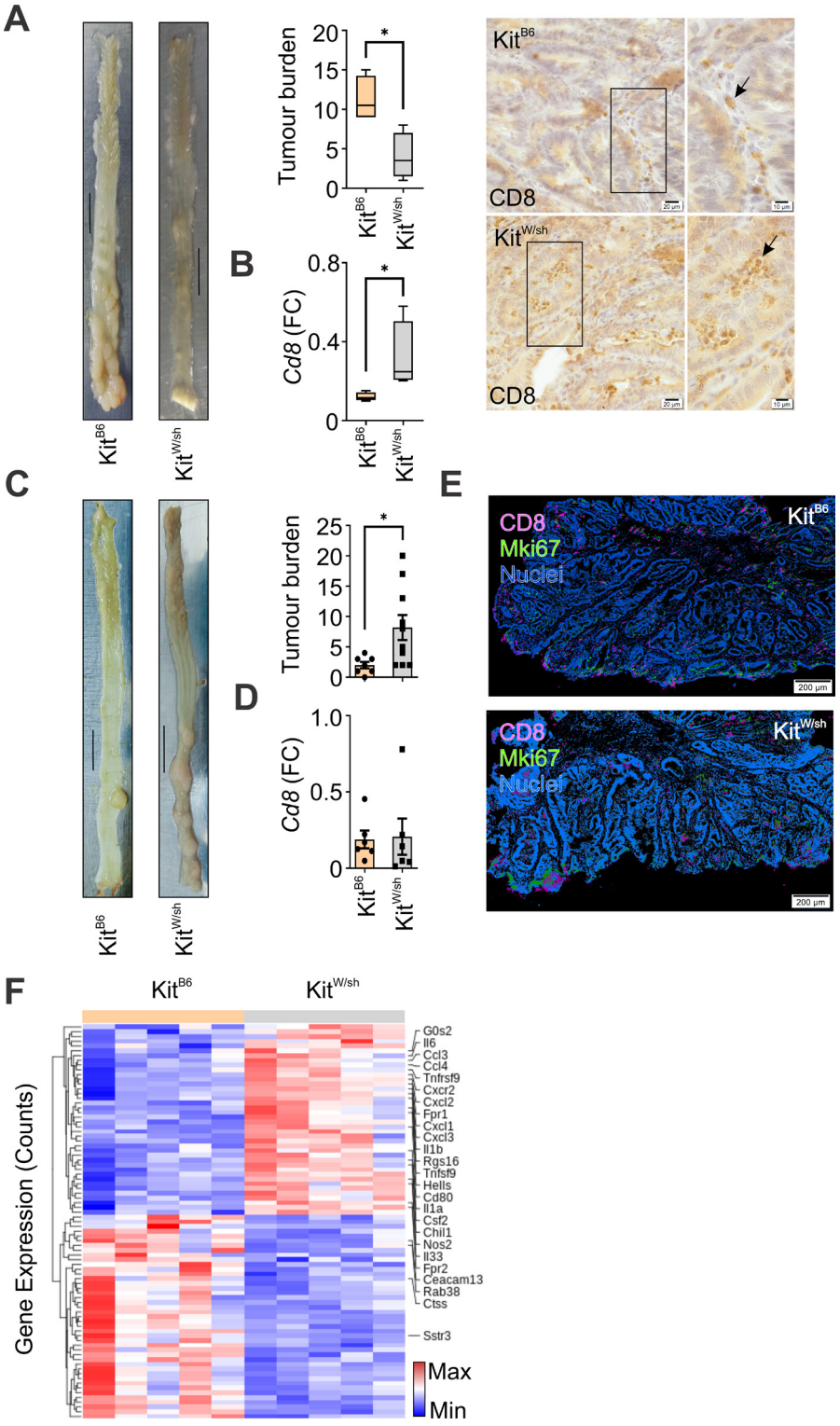

Figure 3 The dual MC role in colorectal tumorigenesis. (A) Representative images of tumors induced by the CA-CRC protocol (Scale bars=1 cm). Graph shows tumor numbers *per* mice (n=8; *p=0.0286). (B) Gene expression analysis for *Cd8* (p=0.0286). Representative images of tumors stained by an anti-CD8 antibody (40× (left-side) and 100× (right-side) magnification; lines indicate 100× magnified areas; arrows lead to positive cells). (C) Representative images of tumors induced by sCRC protocol (Scale bars=1 cm). Graph shows tumor numbers *per* mice (n=17; p=0.0164). (D) Gene expression analysis for *Cd8* (p>0.05). (E) Representative images of multiplex IHC staining for CD8 lymphocytes (CD8) and proliferating tumor cells (Mki67; magnification at 200 µm). Data are shown as the median, highest and lowest values, and upper and lower quartiles (A, B) or individual data points with mean±SEM. (C, D) P values were calculated using two-tailed Mann-Whitney's U test. (F) Heatmap of hierarchical clustering indicates differentially expressed genes (rows) between tumor samples from Kit^{B6} and $Kit^{W/sh}$ mice (n=10). Red indicates upregulation (Max) and blue indicates downregulation (Min). CA-CRC, colitis-associated colorectal cancer; MC, mast cell; sCRC, sporadic CRC.

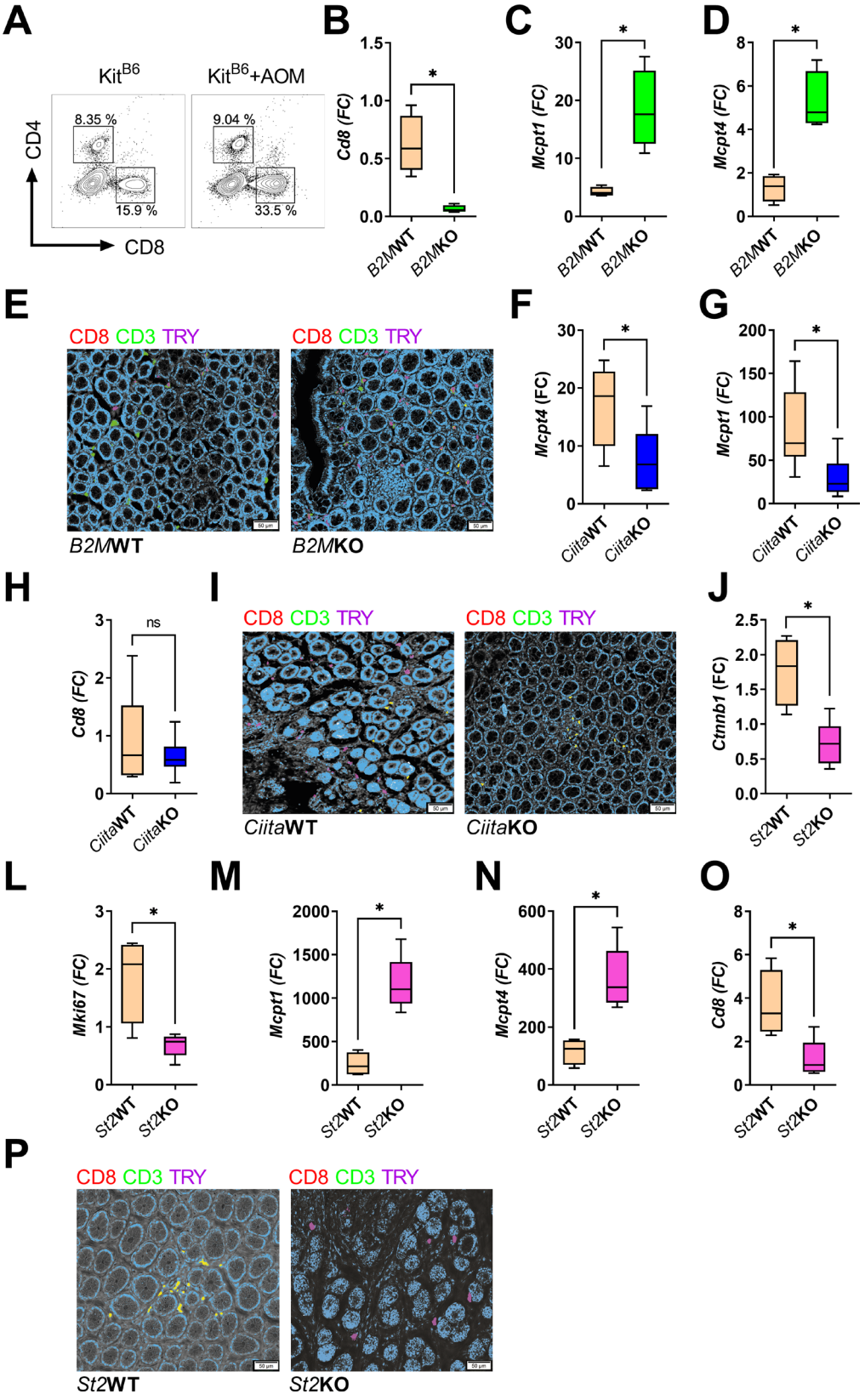

Figure 4 The early colorectal tumorigenic steps require complex immune reactions to develop. (A) Representative dot plot graphs of CD4+ and CD8+ lymphocytes gated for CD45+, live cells, and singlet. (B–D, F, G, J–O) Gene expression analysis for *Cd8* (B, n=8, *p=0.02; H, n=13, p>0.05; O, n=9, *p=0.03), *Mcpt1* (C, n=8, *p=0.02; G, n=13, *p=0.02; M, n=9, *p=0.01), *Mcpt4* (D, n=8, *p=0.02; F, n=13, *p=0.02; N, n=9, *p=0.01), *Ctnnb1* (J, n=9, *p=0.03), and *Mki67* (L, *p=0.03) in *B2M*KO, *Ciita*KO, and *St2*KO mice, and their counterparts. (E, I, P) Representative images of multiplex IHC staining with anti-CD8, anti-CD3, and anti-TRY antibodies (magnification at 50 µm). Data are shown as the median, highest and lowest values, and upper and lower quartiles. P values were calculated using a two-tailed Mann-Whitney's U test. IHC, immunohistochemistry.

lesions in an *Il33r* deficiency model. The *Il33r* deficiency reduced CRC-related biomarkers in carcinogen-exposed mice (figure 4J,L). This condition upregulated expression levels of MC biomarkers but downregulated the gene encoding *Cd8* (figure 4M–P; online supplemental figure 4).

We further confirmed that an MC-lymphocyte axis impacts the development of early tumorigenic lesions in the colon. Thus, these lesions were induced in MC deficient mice and analyzed after 6 weeks from the sixth carcinogenic exposure. This experiment revealed that MC activity reduces the development of early tumorigenic lesions and the levels of *Cd4* and *Cd11c* (figure 5A–C). We further confirmed that increased *Cd4* and *Cd11c* levels were occurring just a week from the sixth carcinogenic exposure (figure 5D–E). Moreover, MC deficiency decreased the expression of a gene associated to an essential DNA damage repair mechanism against AOM-related DNA adducts known as O^6-methylguanine-DNA-methyltransferase (*Mgmt)* (figure 5F).

To further investigate the MC role in these early colon tumorigenic events, we applied our previous reported strategy to study DNA damage and single early tumorigenic events.[22] DNA damage was analyzed following 72 hours from the third carcinogenic exposure to reveal that MC deficiency did not alter the γH2AX levels in the colon while increasing the *Cd11c* expression (figure 5G–H). To study the earliest immunological reactions activated by MC deficiency, we performed transcriptomic analyses in the colon of mice at the third week from the third carcinogenic exposure. Out of several immunological reactions (figure 5I; online supplemental table 6), MC deficiency significantly impacted the inflammatory bowel disease pathway (online supplemental table 7).

We next validated these findings by performing BMT in $Kit^{W/sh}$ mice before inducing the development of single early colon tumorigenic lesions in them (figure 5J). This experiment revealed that restoring MCs into previously MC deficient mice increased proliferation in the carcinogen-exposed colon (*Mki67* (FC), Kit^{B6}BMT – 1.3±0.1; $Kit^{W/sh}$ BMT – 2.9±0.5; p=0.006). Interestingly, rescuing MC activity in MC deficient mice before the development of single early colon tumorigenic lesions increased the Mcpt4 levels while blocking the expression of *Cd11C* (figure 5K,L). These results illustrate that MCs impact and are impacted by other immune reactions activated throughout the development of early colon tumorigenic lesions.

Targeting MCs against CRC lesions

Since our observations suggested that the MC population could promote specific effects in different stages of CRC development, we treated Kit^{B6} mice with CA to inhibit MC activity throughout the 3 weeks of carcinogenic exposure or following this period (figure 6A). Although CA treatment did not alter DNA damage levels (figure 6B), inhibiting MC activity throughout the carcinogenic exposure increased sCRC risk, whereas mice given CA post-carcinogen induction did not develop early tumorigenic lesions (figure 6C). This time-related MC inhibition that promoted the development of early tumorigenic lesions also increased proliferation and upregulated the expression levels of *Cd4*, *Foxp3*, *Cd8*, and *Cd3* (*Cd3* (FC), AOM – 1.3±0.1; AOM+CA – 3.0±0.3; AOM-CA – 2.3±0.7; AOM *vs* AOM+CA, p=0.03; figure 6D,F–H).

We then performed transcriptomic studies to clarify significant changes in inflammatory reactions promoted by pharmacologically inhibiting the MC activity (figure 6I; online supplemental table 8,9). Out of several immunological changes that the CA treatment induces, it inhibited key elements of the cell adhesion pathway (figure 6I**;** online supplemental table 10). Conversely, when CA treatment and carcinogenic exposure are given together, it down-regulates the antigen processing and presentation pathway (online supplemental table 11).

These findings led us to verify how much MCs could impact the engraftment potential of CRC cells. This experiment revealed that MC deficiency blocks the development of CRC allograft tumors without altering their proliferative activity (figure 7A; online supplemental figure 6A). Interestingly, this MC deficiency significantly up-regulates the tumor *Cd4* and *Cd8* expression levels (online supplemental figure 6B). Moreover, it increased the tumor infiltration of CD8 lymphocytes (figure 7B). When we performed an RNAseq analysis to explore potential immune reactions associated with MC deficient tumors, it showed a down-regulation of the proteasome pathway and upregulation of key elements of the antigen processing and presentation mechanism (figure 7C**;** Suppl. online supplemental table 12,13).

Once we tested the therapeutic potential of MC inhibition against CRC development, it revealed that inhibiting MC activity significantly blocks the development of allograft colorectal tumors (figure 7D**;** online supplemental figure 7A). To further explore the anticancer therapeutic potential of MC activity blockade, we observed that CA treatment prevented the growth of melanoma tumor allografts (figure 7E; online supplemental figure 8A,B). Surprisingly, blocking MC activity in melanoma reduced the $CD8^+CD3^+$ T cell population without altering the MC one (figure 7F; online supplemental figure 8C,D). Encouraged by these findings, we blocked MC activity in colorectal tumors 14 days after cancer implantation (online supplemental figure 9A,B). Again, CA treatment inhibited colorectal tumor development and increased the $CD8^+CD3^+$ T cell population without altering the MC numbers (figure 7G–I; online supplemental figure 9C). To challenge the idea that inhibiting MC activity would enhance anticancer response by cytotoxic lymphocytes, we treated CD3-deficient mice with CA for 3 days before implanting MC38 cancer cells. We then monitored the tumor growth for other 11 days. It revealed that without an effective T cell-based response CA treatment did not reduce tumor growth (online supplemental figure 11).

This observation led to testing whether this drug could be combined with a gold-standard chemotherapy

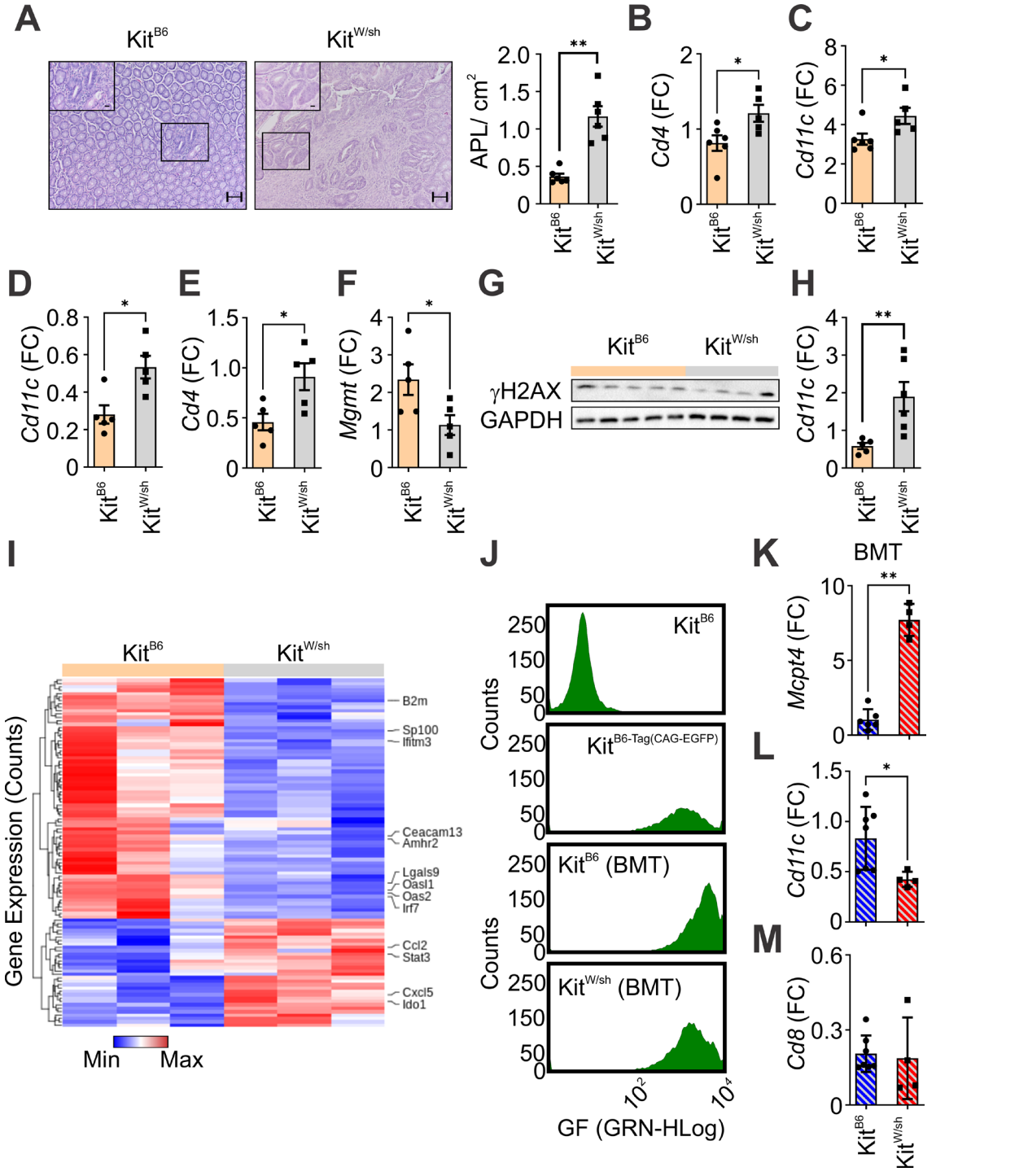

Figure 5 The MC activity protects against early colorectal tumorigenic steps. (A) Representative images (10× and 40× (inset); scale bars=20 µm) of early tumorigenic events preceding the detection of fully grown tumors in the colon. MC deficiency increases the number of them (n=11; *p=0.004). (B, C) Gene expression analysis in colon samples of mice at the sixth week after the sixth carcinogenic exposure for *Cd4* (n=11; *p=0.03) and *Cd11c* (*p=0.03). (D–F) Gene expression analysis in colon samples of mice at the first week after the sixth carcinogenic exposure for *Cd11c* (n=10; *p=0.01), *Cd4* (*p=0.02), and *Mgmt* (n=11; *p=0.04). (G) DNA damage levels by immunoblotting against γH2AX and GADPH in colon samples of mice at the third day after the third carcinogenic exposure. (H) Gene expression analysis for *Cd11c* in colon samples of mice at the third day after the third carcinogenic exposure (n=9; p=0.003). (I) Heatmap of hierarchical clustering obtained from RNA-seq data indicates differentially expressed genes between colon samples of Kit^{B6} and Kit$^{W/sh}$ mice at the third week after the third carcinogenic exposure (n=6). (J) Representative histograms of the BMT protocol performed in both Kit^{B6} and Kit$^{W/sh}$ mice. Spectral color represents EGFP^{+} cells by fluorescence intensity (GF; *x* axis) and cell counting (*y* axis) in different experimental conditions. (K–M) Gene expression analysis for *Mcpt4* (*p=0.004), *Cd11c* (**p=0.01), and *Cd8* (p>0.05) in colon samples of mice at the third week after the third carcinogenic exposure following the BMT procedure. Data are shown as individual data points with mean±SEM p value was calculated using a two-tailed Mann-Whitney's U test. BMT, bone marrow transplantation.

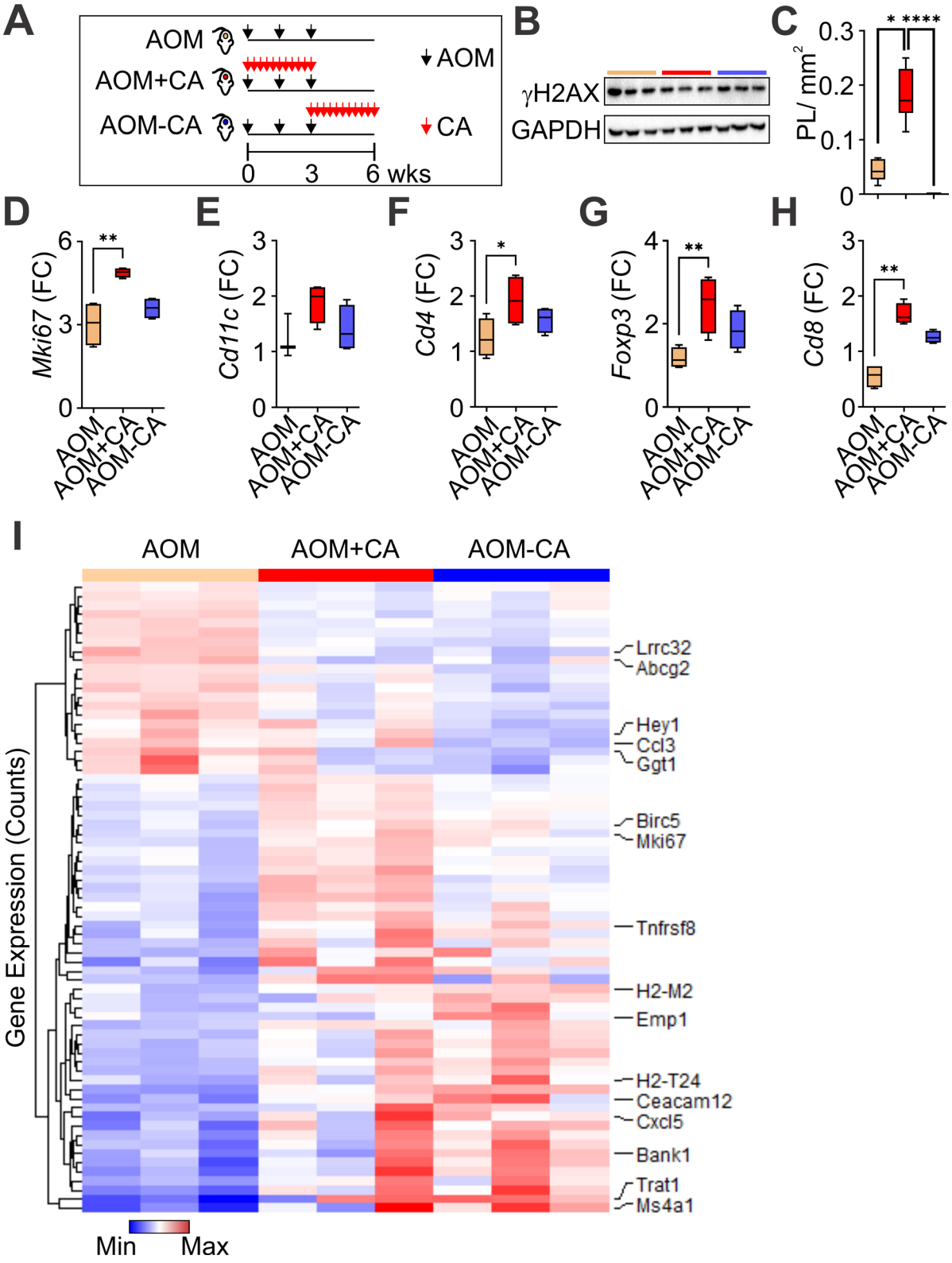

Figure 6 The MC activity impacts the development of early tumorigenic lesions in the colon. (A) Timeline for different groups treated with CA (red arrows) and AOM (black arrows) throughout 6 weeks. (B) DNA damage levels by immunoblotting against γH2AX and GADPH in colon samples. (C) Inhibiting MC activity in specific timepoints of carcinogenic exposure can either promote or inhibit the development early tumorigenic events in the colon (n=24; *p=0.042, ****p<0.0001). (D–H) Gene expression analysis for *Mki67* (n=24; *p<0.01; AOM vs AOM+CA), *Cd11c* (p>0.05), *Cd4* (*p<0.05; AOM *vs* AOM+CA), *Foxp3* (*p<0.01; AOM vs AOM+CA), and *Cd8* (*p<0.01; AOM vs AOM+CA). Data are shown as the median, highest and lowest values, and upper and lower quartiles (C–H). P values were calculated using ANOVA with a Kruskal-Wallis' post hoc test. (I) Heatmap of hierarchical clustering obtained from RNA-seq data indicates differentially expressed genes (n=12). ANOVA, analysis of variance; AOM, azoxymethane; CA, colitis-associated; MC, mast cell.

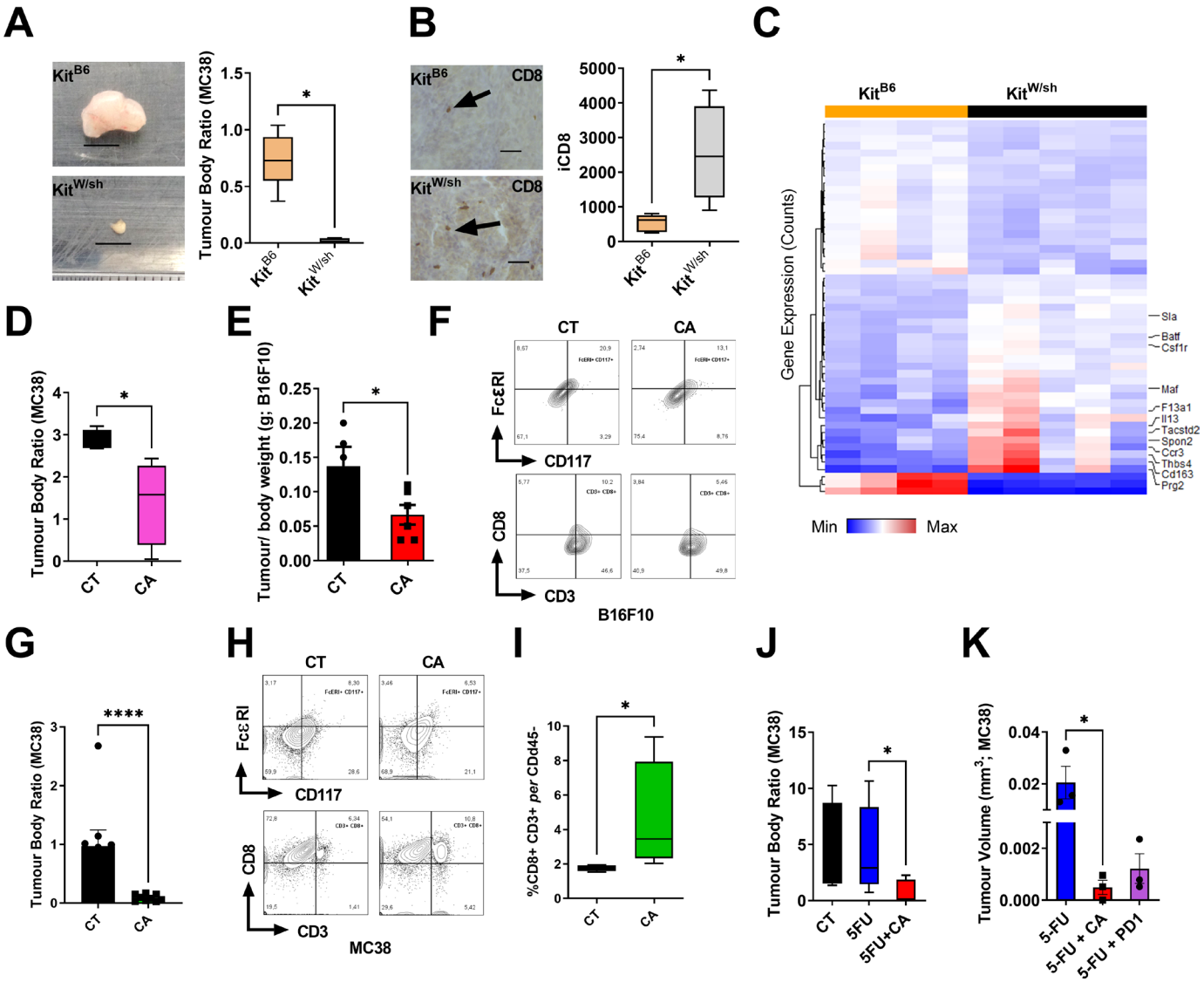

Figure 7 The MC activity can be therapeutically targeted against CRC in mice. (A) Representative images of tumors following harvest (scale bars=1 cm). The volume of allograft tumors were analyzed after 14 days from their subcutaneous implantation (n=9; *p=0.01). (B) Representative images of CD8+ cells stained by anti-CD8 antibody (40× magnification; scale bars=30 µm; arrows lead to positive cells). MC deficiency promotes CD8+ cell infiltration in tumors (n=9, *p=0.01). (C) Heatmap of hierarchical clustering obtained from RNA-seq data indicates differentially expressed genes (n=9). (D) Relative tumor volume between CA-treated (CA) and untreated (CT) mice at the last day of a 15-days experiment (n=8; *p=0.02). (E) Relative tumor volume between CA-treated and untreated mice bearing melanoma tumors at the last day of a 15-days experiment (n=11; *p=0.04). (F, H) Representative dot plot graphs of MCs (CD45+CD117+FcεRI+) and CD45+CD8+CD3+ T cells isolated from B16F10 tumor samples. (G) Relative tumor volume between CA-treated and untreated mice bearing CRC tumors at the last day of a 26-days experiment (n=17; ****p<0.0001). (I) Graphs show percentages of $CD45^{+}CD8^{+}CD3^{+}$ T cells isolated from tumor samples (n=8; *p=0.02). (J, K) Relative tumor growth among untreated, 5-FU-treated, and combined treatments with 5-FU for 17 days (J, n=15; *p=0.04; K, n=9; *p=0.04). Data are shown as the median, highest and lowest values, and upper and lower quartiles, or individual data points with mean±SEM p values were calculated using two-tailed Mann-Whitney's U test and ANOVA with a Kruskal-Wallis' post hoc test. 5-FU, 5-fluorouracil; ANOVA, analysis of variance; CA, colitis-associated; CRC, colorectal cancer; MCs, mast cells.

in CRC treatment. We found that CA potentialized the anticancer effects of 5-FU (figure 7J; online supplemental figure 7B). Nevertheless, the results of this combination therapy seem to be comparable to the association of chemotherapy with a standard immunotherapeutic antibody (figure 7K). Our data demonstrate that MCs impact the multistage development of CRC and are a druggable target against this disease.

DISCUSSION

In this study, we have shown that MCs play an intricate role in CRC development in human patients. Tan *et al* reported that a low MC counting correlates with more invasive tumors, increased number of metastatic lesions, and reduced 5 year survival rates.[33] Another study with 72 cases of CRC showed that a high MC density could promote overall survival and reduce the risk of malignancy-related

deaths.[7] A randomized study with 82 cases of colorectal liver metastases has shown that chemotherapy increases MC density. This study also demonstrated that high MC numbers correlates with tumor regression and progression free survival.[34]

Contrary, Malfettone *et al* have shown that a reduced MC population improves the prognosis of CRC patients while increasing this cell density worsens the outcome of the disease.[5] Also, Nielsen *et al* reported that increased MC numbers in a tumor might be related to better patient survival rates.[8] Mao *et al* also showed in 854 subjects that a high MC counting may lead to poor overall patient survival. However, the authors also found that a high MC number may improve the patient survival in cases of stages II and III not receiving adjuvant chemotherapy. They further showed that MC density alters the CD8 T cell population.[6] Our findings suggest that MC populations closely interacts with tumor-infiltrating lymphocytes.

Our mouse-based dataset provides significant evidence that MCs could either promote or inhibit the development of colon tumors. Although tumor-primed MCs seemed to have some anticancer activity in a co-culture system, our in vivo experiments suggest that the MC effects can vary according to the type of stimuli promoting CRC. Whereas MCs would inhibit CD8 cell density but promote inflammation-related CRC (CA-CRC), they may be protective against the DNA damage-related form of this disease (sCRC). In a *Kit* mutant mouse strain other than the $Kit^{W/sh}$ one (differences described by Grimbaldeston *et al*[35]), Wedemeyer and Galli reported that MC deficiency reduced carcinogen-induced colorectal tumor burden.[9] We have also observed that $Kit^{W/sh}$ and $Kit^{W/W\text{-}v}$ respond differently to the same carcinogen exposure (figures 3A and 5A and online supplemental figure 11).

Sinnamon *et al* reported that deleting adenomatous polyposis coli (*Apc*) in mice promotes TRY expression in tumors. By ablating the MC population in $Apc^{Min/+}$ mice, they found that MC activity blocked tumor development.[14] Bodduluri *et al* have also shown that chemokine-mediated MC recruitment initiates MC-derived leukotriene-regulated CD8+T cell homing and antitumor immunity reducing intestinal tumor burden in $Apc^{Min/+}$ mice.[13] In the CA-CRC model, Tanaka *et al* reported that MC deficient mice are less susceptible to inflammation-associated colorectal tumors.[12] Rigoni *et al* also observed that MC deficiency increased the number of malignant lesions in the colon.[11]

We further demonstrated that MC activity alters pivotal immune mechanisms and vice-versa. Whether MC density seemed to determine the growth potential of carcinogen-induced lesions (figures 3, 5 and 6), an effect completely reversed in cancer (figure 7), essential immune factors also changed the MC activity. The balance between MHCI and MHCII levels altered MC-related chemokines release in our study. Le Bouteiller *et al* found that anti-MHC alloantibodies modulate MC activity.[36] When MCs were stimulated by antibody bipolar bridging, Daeron and Voisin showed that MHC-I reverse signaling modulates MC activity.[37 38] Moreover, Malbec *et al* revealed that antigen recognition by FcγR-bound IgG on MCs could mediate transinhibition without co-clustering with FcεRI binding to IgE antibodies, a mechanism inhibiting oncogen-induced proliferation in mastocytoma.[39] Furthermore, MCs seem able to express MHCII in cell culture but not in vivo.[1 40] Then, Dudeck *et al* showed that innate-to-innate synapse-like contacts enable DC-to-MC molecule transfers including MHCII proteins and subsequent T cell priming.[41]

The Il6-related and Il33r-related signaling promoted opposing effects on MC activity during the early colon tumorigenic steps. Desai *et al* have shown that Il6 stimulation expands MC population and promotes its reactivity.[42] It has been demonstrated that that differentiating CD34+ human cord blood cells into MCs requires stem cell factor stimulation but adding IL6 increases cell size and intracellular levels of chymase and histamine.[43] In both human CRC and mouse polyposis, MCs can modulate and be modulated by Il10, Il6, Il17, and Il2 levels, by which they recruit Treg and promote Treg-induced suppression of host-vs-graft rejection responses or render the Treg proinflammatory role furthering CRC development.[44] Interestingly, Il33r seems required for CRC cellular expansion,[45] while Il33 deficiency inhibited intestinal tumor burden and reduced intratumor MC density and MC-derived proteases and cytokines release.[46 47] Moreover, Il11-induced tumor-derived Il33 signaling activates MCs and promotes gastric cancer development in mice. Genetically ablating Il33r blocks MC-dependent recruitment of macrophages limiting tumor growth.[48]

We further explored the idea that MCs are druggable targets against CRC. Pharmacologically inhibiting MC activity blocks tumor growth and can be combined with standard chemotherapy strategies. Pharmacologically inhibiting MCs activity has been shown an effective anticancer strategy against different types of tumors.[10 49–51] Moreover, drug-based MC inhibition has been combined with gemcitabine, decreasing pancreatic cancer's tumor growth.[50] Also, it has also been associated with anti-angiogenic therapy to treat murine lymphoma and pancreatic cancer.[51] These facts illustrate that MCs are a druggable target that can potentialize the anticancer effects of current therapies. However, a potential limitation of our study is that in addition to inhibiting MC activity CA can impact cancer cell signaling and survival as well as other immune responses.[52 53] The fact that CA treatment requires T lymphocytes to block tumor growth and can be combined with 5-FU strengthens the idea that CRC patients may can benefit from MC-based therapies.

Therefore, we suggest that MC activity can significantly impact CRC development in either a beneficial or harmful fashion; this effect seems to be substantially determined during the early stages of this disease. Moreover, this MC activity appears to be a druggable target with significant potential for anti-CRC therapeutic strategies.

Author affiliations
[1]Department of Clinical Analyses, Toxicology and Food Sciences, Faculty of Pharmaceutical Sciences of Ribeirão Preto, University of São Paulo, Ribeirao Preto, Brazil
[2]Department of Biochemistry and Immunology, University of Sao Paulo, Sao Paulo, Brazil
[3]Department of Toxicology, Bromatology, and Clinical Analysis, University of Sao Paulo, Sao Paulo, Brazil
[4]Department of Clinical Medicine, University of Sao Paulo, Sao Paulo, Brazil
[5]Department of Pathology and Forensic Medicine, University of Sao Paulo, Sao Paulo, Brazil
[6]Hemotherapy Center of Ribeirao Preto, Ribeirao Preto, Brazil
[7]Department of Clinical Medicine, Federal University of Minas Gerais, Belo Horizonte, Brazil
[8]Department of Pharmacology, University of Sao Paulo, Sao Paulo, Brazil
[9]Department of Cell and Molecular Biology, Virology Research Center, University of Sao Paulo, Ribeirao Preto, Brazil
[10]Pharmacology and Toxicology, University of Toronto, Toronto, Ontario, Canada
[11]Nutrition, University of Oslo, Oslo, Norway
[12]Medical Imaging, Hematology, and Oncology, University of Sao Paulo, Sao Paulo, Brazil
[13]Biocel Ltd, Hull, UK
[14]Department of Cellular Pathology, Blackpool Teaching Hospitals NHS Foundation Trust, Blackpool, UK

Contributors Study concept and design: VK; Acquisition of data: JYS, JEO, LYA, ESS, MOB, TMM, SA, CLAS, DC, MVA, VLD, SBG, FQC, GCMC, RBM, LMC, FLM, SAU, VK; Statistical analysis: JYS, JEO, TMM, GCMC, VK; Analysis and interpretation of data: All; Drafting the first version of the manuscript: JYS and VK; Critical revision of the manuscript: All; Obtained funding: DC, TMM, MOB, VLDB, FQC, JM, LMC, FLM, SAU, VK; Technical and material support: LYA, MOB, SA, CLAS, DC, VLDB, RBM, MAV, SBG, FQC, JM, LMC, SAU, VK; Study supervision and guarantor: SAU, VK.

Funding The authors disclose receipt of the following financial support for the development of this investigation: Sao Paulo Research Foundation (FAPESP; 2014/06428-5 and 2018/00583-0), and the Foundation for Support to Teaching, Research and Assistance of the Hospital das Clínicas of the Faculty of Medicine of Ribeirão Preto, University of São Paulo (FAEPA).

Disclaimer The funder had no role in the study design, data collection, analysis, decision to publish, or preparation of the manuscript.

Competing interests None declared.

Patient consent for publication Not applicable.

Ethics approval The Research Ethics Committee of the Clinical Hospital of the Ribeirao Preto School of Medicine of the University of São Paulo approved the use of matching malignant and healthy human tissue samples of nineteen CRC cases (38 samples in total; 19 healthy colon tissues and 19 CRC tissues) from the surgical tissue bank (12873/2014).

Provenance and peer review Not commissioned; externally peer reviewed.

Data availability statement Data are available on reasonable request.

ORCID iDs
Sergio Albuquerque http://orcid.org/0000-0003-2530-9226
Vinicius Kannen http://orcid.org/0000-0001-6290-8063

REFERENCES

1 Chatterjee V, Gashev AA. Mast cell-directed recruitment of MHC class II positive cells and eosinophils towards mesenteric lymphatic vessels in adulthood and elderly. *Lymphat Res Biol* 2014;12:37–47.
2 Villa I, Skokos D, Tkaczyk C, *et al*. Capacity of mouse mast cells to prime T cells and to induce specific antibody responses in vivo. *Immunology* 2001;102:165–72.
3 Frandji P, Tkaczyk C, Oskeritzian C, *et al*. Exogenous and endogenous antigens are differentially presented by mast cells to CD4+ T lymphocytes. *Eur J Immunol* 1996;26:2517–28.
4 Dimitriadou V, Mécheri S, Koutsilieris M, *et al*. Expression of functional major histocompatibility complex class II molecules on HMC-1 human mast cells. *J Leukoc Biol* 1998;64:791–9.
5 Malfettone A, Silvestris N, Saponaro C. High density of tryptase-positive mast cells in human colorectal cancer: a poor prognostic factor related to protease-activated receptor 2 expression. *J Cell Mol Med* 2013;17:1025–37.
6 Mao Y, Feng Q, Zheng P, *et al*. Low tumor infiltrating mast cell density confers prognostic benefit and reflects immunoactivation in colorectal cancer. *Int J Cancer* 2018;143:2271–80.
7 Mehdawi L, Osman J, Topi G, *et al*. High tumor mast cell density is associated with longer survival of colon cancer patients. *Acta Oncol* 2016;55:1434–42.
8 Nielsen HJ, Hansen U, Christensen IJ, *et al*. Independent prognostic value of eosinophil and mast cell infiltration in colorectal cancer tissue. *J Pathol* 1999;189:487–95.
9 Wedemeyer J, Galli SJ. Decreased susceptibility of mast cell-deficient Kit(W)/Kit(W-v) mice to the development of 1, 2-dimethylhydrazine-induced intestinal tumors. *Lab Invest* 2005;85:388–96.
10 Motawi TK, El-Maraghy SA, ElMeshad AN, *et al*. Cromolyn chitosan nanoparticles as a novel protective approach for colorectal cancer. *Chem Biol Interact* 2017;275:1–12.
11 Rigoni A, Bongiovanni L, Burocchi A, *et al*. Mast cells infiltrating inflamed or transformed gut alternatively sustain mucosal healing or tumor growth. *Cancer Res* 2015;75:3760–70.
12 Tanaka T, Ishikawa H. Mast cells and inflammation-associated colorectal carcinogenesis. *Semin Immunopathol* 2013;35:245–54.
13 Bodduluri SR, Mathis S, Maturu P, *et al*. Mast Cell-Dependent $CD8^+$ T-cell Recruitment Mediates Immune Surveillance of Intestinal Tumors in $Apc^{Min/+}$ Mice. *Cancer Immunol Res* 2018;6:332–47.
14 Sinnamon MJ, Carter KJ, Sims LP, *et al*. A protective role of mast cells in intestinal tumorigenesis. *Carcinogenesis* 2008;29:880–6.
15 Newman AM, Liu CL, Green MR, *et al*. Robust enumeration of cell subsets from tissue expression profiles. *Nat Methods* 2015;12:453–7.
16 Thorsson V, Gibbs DL, Brown SD, *et al*. The immune landscape of cancer. *Immunity* 2019;51:411–2.
17 Townsend MJ, Fallon PG, Matthews DJ, *et al*. T1/ST2-deficient mice demonstrate the importance of T1/ST2 in developing primary T helper cell type 2 responses. *J Exp Med* 2000;191:1069–76.
18 Carlos D, Sá-Nunes A, de Paula L, *et al*. Histamine modulates mast cell degranulation through an indirect mechanism in a model IgE-mediated reaction. *Eur J Immunol* 2006;36:1494–503.
19 Wargovich MJ, Chen CD, Jimenez A, *et al*. Aberrant crypts as a biomarker for colon cancer: evaluation of potential chemopreventive agents in the rat. *Cancer Epidemiol Biomarkers Prev* 1996;5:355–60.
20 Kubota T, Fujita S, Kodaira S. Antitumor activity of fluoropyrimidines and thymidylate synthetase inhibition. *Jpn J Cancer Res* 1991;82:476–82.
21 Neufert C, Becker C, Neurath MF. An inducible mouse model of colon carcinogenesis for the analysis of sporadic and inflammation-driven tumor progression. *Nat Protoc* 2007;2:1998–2004.
22 Sakita JY, Bader M, Santos ES, *et al*. Serotonin synthesis protects the mouse colonic crypt from DNA damage and colorectal tumorigenesis. *J Pathol* 2019;249:102–13.
23 Finnberg NK, Hart LS, Dolloff NG, *et al*. High-resolution imaging and antitumor effects of GFP(+) bone marrow-derived cells homing to syngeneic mouse colon tumors. *Am J Pathol* 2011;179:2169–76.
24 Leite CA, Mota JM, de Lima KA, *et al*. Paradoxical interaction between cancer and long-term postsepsis disorder: impairment of de novo carcinogenesis versus favoring the growth of established tumors. *J Immunother Cancer* 2020;8:e000129.
25 Ravindran A, Rönnberg E, Dahlin JS, *et al*. An optimized protocol for the isolation and functional analysis of human lung mast cells. *Front Immunol* 2018;9:2193.
26 Puck TT, Marcus PI. A rapid method for viable cell titration and clone production with HeLa cells in tissue culture: the use of x-irradiated cells to supply conditioning factors. *Proc Natl Acad Sci U S A* 1955;41:432–7.

27 Samoszuk M, Tan J, Chorn G. Clonogenic growth of human breast cancer cells co-cultured in direct contact with serum-activated fibroblasts. *Breast Cancer Res* 2005;7:R274–83.
28 Puebla-Osorio N, Sarchio SNE, Ullrich SE, *et al*. Detection of infiltrating mast cells using a modified toluidine blue staining. *Methods Mol Biol* 2017;1627:213–22.
29 Love MI, Huber W, Anders S. Moderated estimation of fold change and dispersion for RNA-Seq data with DESeq2. *Genome Biol* 2014;15:550.
30 Computing RFfS. *A language and environment for statistical computing*, 2021.
31 Koller BH, Marrack P, Kappler JW, *et al*. Normal development of mice deficient in beta 2M, MHC class I proteins, and CD8+ T cells. *Science* 1990;248:1227–30.
32 Xing W, Austen KF, Gurish MF, *et al*. Protease phenotype of constitutive connective tissue and of induced mucosal mast cells in mice is regulated by the tissue. *Proc Natl Acad Sci U S A* 2011;108:14210–5.
33 Tan S-Y, Fan Y, Luo H-S, *et al*. Prognostic significance of cell infiltrations of immunosurveillance in colorectal cancer. *World J Gastroenterol* 2005;11:1210–4.
34 Tanis E, Julié C, Emile J-F, *et al*. Prognostic impact of immune response in resectable colorectal liver metastases treated by surgery alone or surgery with perioperative FOLFOX in the randomised EORTC study 40983. *Eur J Cancer* 2015;51:2708–17.
35 Grimbaldeston MA, Chen C-C, Piliponsky AM, *et al*. Mast cell-deficient W-sash c-kit mutant kit W-sh/W-sh mice as a model for investigating mast cell biology in vivo. *Am J Pathol* 2005;167:835–48.
36 Le Bouteiller P, Daëron M, Duc HT, *et al*. An ultrastructural study of two different responses of mouse mast cells to transplantation antibodies directed against the same transplantation antigens. *Eur J Immunol* 1976;6:326–32.
37 Daëron M, Voisin GA. H-2 antigens, on mast cell membrane, as target antigens for anaphylactic degranulation. *Cell Immunol* 1978;37:467–72.
38 Daëron M, Voisin GA. Mast cell membrane antigens and Fc receptors in anaphylaxis. I. products of the major histocompatibility complex involved in alloantibody-induced mast cell activation. *Immunology* 1979;38:447–58.
39 Malbec O, Cassard L, Albanesi M, *et al*. Trans-inhibition of activation and proliferation signals by Fc receptors in mast cells and basophils. *Sci Signal* 2016;9:ra126.
40 Kambayashi T, Allenspach EJ, Chang JT, *et al*. Inducible MHC class II expression by mast cells supports effector and regulatory T cell activation. *J Immunol* 2009;182:4686–95.
41 Dudeck J, Medyukhina A, Fröbel J, *et al*. Mast cells acquire MHCII from dendritic cells during skin inflammation. *J Exp Med* 2017;214:3791–811.
42 Desai A, Jung M-Y, Olivera A, *et al*. Il-6 promotes an increase in human mast cell numbers and reactivity through suppression of suppressor of cytokine signaling 3. *J Allergy Clin Immunol* 2016;137:1863–71.
43 Conti P, Kempuraj D, Di Gioacchino M, *et al*. Interleukin-6 and mast cells. *Allergy Asthma Proc* 2002;23:331–5.
44 Blatner NR, Bonertz A, Beckhove P, *et al*. In colorectal cancer mast cells contribute to systemic regulatory T-cell dysfunction. *Proc Natl Acad Sci U S A* 2010;107:6430–5.
45 O'Donnell C, Mahmoud A, Keane J, *et al*. An antitumorigenic role for the IL-33 receptor, ST2L, in colon cancer. *Br J Cancer* 2016;114:37–43.
46 Maywald RL, Doerner SK, Pastorelli L, *et al*. Il-33 activates tumor stroma to promote intestinal polyposis. *Proc Natl Acad Sci U S A* 2015;112:E2487–96.
47 He Z, Chen L, Souto FO, *et al*. Epithelial-derived IL-33 promotes intestinal tumorigenesis in Apc $^{Min/+}$ mice. *Sci Rep* 2017;7:5520.
48 Eissmann MF, Dijkstra C, Jarnicki A, *et al*. IL-33-mediated mast cell activation promotes gastric cancer through macrophage mobilization. *Nat Commun* 2019;10:2735.
49 Johnson C, Huynh V, Hargrove L, *et al*. Inhibition of mast cell-derived histamine decreases human cholangiocarcinoma growth and differentiation via c-Kit/stem cell factor-dependent signaling. *Am J Pathol* 2016;186:123–33.
50 Arumugam T, Ramachandran V, Logsdon CD. Effect of cromolyn on S100P interactions with RAGE and pancreatic cancer growth and invasion in mouse models. *J Natl Cancer Inst* 2006;98:1806–18.
51 Wroblewski M, Bauer R, Cubas Córdova M, *et al*. Mast cells decrease efficacy of anti-angiogenic therapy by secreting matrix-degrading granzyme B. *Nat Commun* 2017;8:269.
52 Motawi TMK, Bustanji Y, El-Maraghy S, *et al*. Evaluation of naproxen and cromolyn activities against cancer cells viability, proliferation, apoptosis, p53 and gene expression of survivin and caspase-3. *J Enzyme Inhib Med Chem* 2014;29:153–61.
53 Puzzovio PG, Brüggemann TR, Pahima H, *et al*. Cromolyn sodium differentially regulates human mast cell and mouse leukocyte responses to control allergic inflammation. *Pharmacol Res* 2022;178:106172.